

## 4. EXPERIMENTAL FACILITIES IN BEAM HALL

### 4.1 GPSC & NEUTRON DETECTOR ARRAY FACILITY

N. Saneesh, K.S. Golda, A. Jhingan and P. Sugathan

The NAND detectors have been tested thoroughly for neutron-gamma discrimination and light output integrating capability. Installation of the vacuum components, beam dump shielding, etc. has been completed. The facility has been tested with in-beam experiment, by collecting signals from all 100 detectors. VME-based data acquisition has been used for readout of signal parameters of all neutron detectors, in coincidence with fission fragments.

User experiments have been performed using  $^{48}\text{Ti}$  beam from Pelletron-LINAC accelerator facility. A pair of multi-wire proportional counters (MWPC) was mounted at folding angles, in the reaction plane, for simultaneous detection of fission fragments. The objective of the user experiments in NAND facility was to study the dynamics of fission of very heavy systems by probing mass-gated neutron multiplicity. User experiments in GPSC used the charged particle detector array, HYTAR (HYbrid Telescope ARray), for measurement of angular distributions of fission fragments and quasi-elastic scattering.

Following experiments have been carried out in NAND and GPSC facilities during the year.

Sl. No.	User	System	Duration	Facility
1	Panjab University	$^{48}\text{Ti} + ^{144,154}\text{Sm}$	June 09–19, 2015	NAND
2	Panjab University	$^{48}\text{Ti} + ^{208}\text{Pb}$	June 20–25, 2015	NAND
3	Panjab University	$^{48}\text{Ti} + ^{232}\text{Th}$	July 07 – 17, 2015	NAND

#### 4.1.1 Measurement of neutron cross-talk as a function of distance (angle) in NAND array

N. Saneesh, A. Jhingan and P. Sugathan

In any large neutron detector array, neutrons can scatter from neighbouring detectors and cause cross-talk between detectors. When a scattered neutron, after depositing a minimum amount of energy in one detector cell, interacts with another cell, the event is called a false coincidence or a cross-talk. Cross-talk depends on incident neutron energy, distance between the detectors and detector dimensions. For a multi-neutron detector array like NAND, cross-talk is inevitable and it is desirable to quantify the cross-talk events for better understanding of physical processes.

We performed an off-line test to estimate the cross-talk in the NAND array using neutrons from Am-Be source. To measure the cross-talk probability, which is the ratio of number of cross-talk events to number of true coincidences, we have considered a reference detector at the centre and its 15 neighbouring detectors in two rings, having radii 55 cm and 94 cm with respect to the centre. The neutron detection threshold in each cell was set for 120 keV light output equivalent using a  $^{137}\text{Cs}$  gamma source. The Am-Be source emits one neutron and a gamma ray per decay event. This source was mounted at the centre of the geodesic dome shaped array and a pair of NaI detectors was used for associated gamma ray detection (Figure 4.1.1). Neutron detector signals were collected in event mode by setting up coincidence between the reference neutron detector signal and signal from either of the NaI detector as the master gate for data collection. As the background neutron flux is negligible, an event with a neutron in the reference detector and gamma ray in NaI can be considered as a true event. In addition, as the source emits only one neutron per event, a neutron in any of the surrounding detectors along with a neutron in the reference detector is assumed to be due to cross-talk.

Pulse Shape Discrimination (PSD) based on conventional zero cross method was used for neutron-gamma

separation. True coincidence events triggered by neutrons were identified from the PSD v/s TOF correlation plot from the central detector. The neutrons identified in the reference detector were applied as software gate in two dimensional plots (between PSD and TOF) of other detectors to count cross-talk events. After the analysis, the cross-talk probability was estimated to be  $4.61 \times 10^{-4}$  with less than 6% error for the first ring of detectors at 55 cm and  $1.12 \times 10^{-4}$  with less than 13 % error for the second ring at 94 cm from the reference detector.

The result was compared with cross-talk simulation performed using FLUKA, the multi-particle transport code. The geometrical setup used for simulation is shown in Figure 4.1.2. An event-by-event binning of neutrons in the reference detector was performed and the number of neutrons in the surrounding detectors were counted. Simulated data were analyzed to extract cross-talk probability and it was found to be matching with the measured values.



Fig. 4.1.1: The set-up used for measurement of cross-talk in NAND array. Two NaI detectors are mounted close to the source kept inside the chamber.

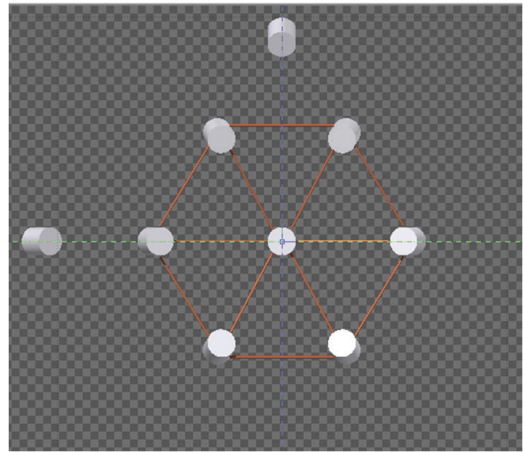


Fig. 4.1.2: Geometry used in simulation. The reference detector at the centre and the first ring of detectors is shown. The two detectors shown at far positions are part of the second ring.

#### 4.1.2 Simulation of neutron detector response to mono-energetic gamma rays

N. Saneesh, A. Jhingan and P. Sugathan

The light output response of BC501 neutron detector was simulated using FLUKA, a fully integrated Monte Carlo code for simulating particle interaction and transport in a material medium. Modelling of various physical processes and the reliability of data from library used in any simulation package can be evaluated well by comparing the simulated results to experimentally measured quantities. This procedure will, in turn, help in evaluating the response parameters of the detectors such as light output resolution and geometrical dependence for further applications of the simulation package. One of the best candidates for this purpose is the pulse height spectrum from mono-energetic gamma rays.

The mono-energetic gamma rays from  $^{22}\text{Na}$  (511 keV) were used for comparison. Background triggering of neutron detectors was minimized by setting a coincidence condition in data collection using a NaI detector. The geometrical constraints, such as detector dimension, source to detector distance, solid angle etc., were considered in the simulation, as well. The corresponding geometrical set-up is shown in Figure 4.1.3. To compare the simulated data with experimental pulse height spectrum, the light output resolution has to be incorporated. This has been done by folding the simulated data with a Gaussian distribution having FWHM equal to light output resolution,  $\Delta L$ . The light output resolution has been parameterized as

$$\frac{\Delta L}{L} = \sqrt{\alpha^2 + \frac{\beta^2}{L} + \frac{\gamma^2}{L^2}}$$

where the coefficients  $\alpha$ ,  $\beta$  and  $\gamma$  are derived by comparing the simulation with experimental data. Fig. 4.1.4 shows the fit to the experimental data obtained by using optimized set of parameters. With this parameter set, pulse height simulation has been compared with experimental data for a different gamma energy and the result was found to be in good agreement. The matching of experimental data with simulation proves the reliability of the package for light output simulations.

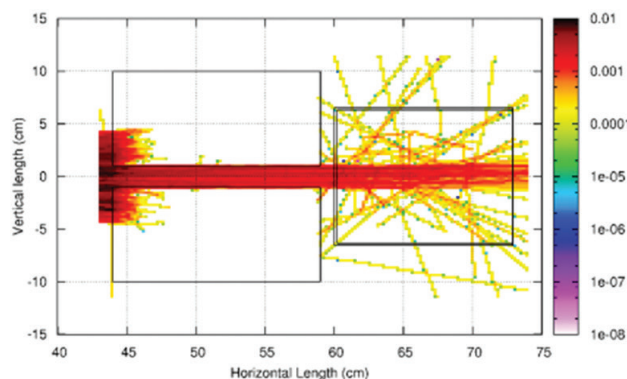


Fig. 4.1.3: Geometrical set-up for FLUKA simulation. The source was positioned 60 cm away from the detector and the beam collimation has been done with thick lead blocks to illuminate the detector selectively. Colour code shows the spatial distribution of gamma ray fluence.

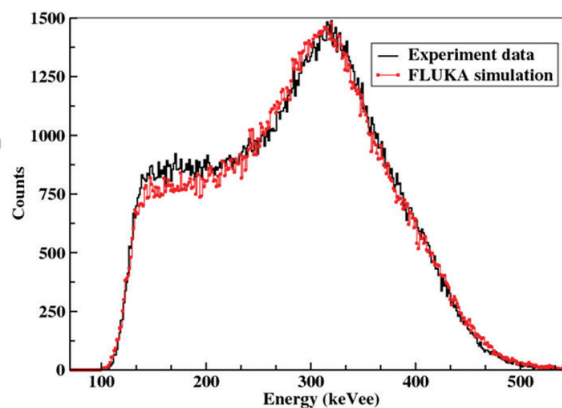


Fig. 4.1.4: Comparison of experimental light output spectrum (black line) from BC501A for 511 keV gamma rays with FLUKA simulation (red line) for 120 keVee threshold.

## 4.2 GAMMA DETECTOR ARRAYS

### 4.2.1 Installation of INGA

R. K. Gurjar, Indu Bala, Kusum Rani, S. Bhattacharjee, R. Garg, S. Muralithar, R. P. Singh and students from universities and institutes

In the last academic year, major effort was put to install the Indian National Gamma Array (INGA) detectors in the INGA-HYRA beam line. Fourteen Clover and anti-Compton shields were tested and installed in the INGA setup. The detectors were mounted on the back hemisphere of the INGA mechanical support. This was done to enable coupling of INGA with the HYbrid Recoil mass Analyzer (HYRA) for coupled mode operation. The  $\text{LN}_2$  filling system was revived and tested for continuous operation. The IUAC Clover modules were used for pulse processing and were tested for prolonged operation. CAMAC based data acquisition system was tested with three CAMAC crates in cascade. Figure 4.2.1 shows a picture of the INGA setup during the test run.

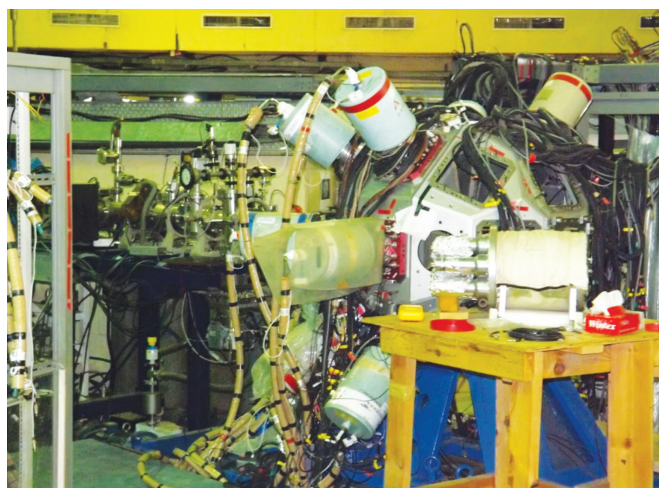


Fig. 4.2.1: INGA setup during the test run in April 2016. Fourteen Clover detectors were mounted on the back hemisphere of the INGA stand.

#### 4.2.1.1 Earthing in INGA

New earthing pits were drilled in the concrete floor to provide clean ground for sensitive electronics equipment. All the nineteen inch racks which house the electronics in the data acquisition room and all the CAMAC crates and NIM bins were connected to clean ground using copper bars and wires as shown in Figure 4.2.2.

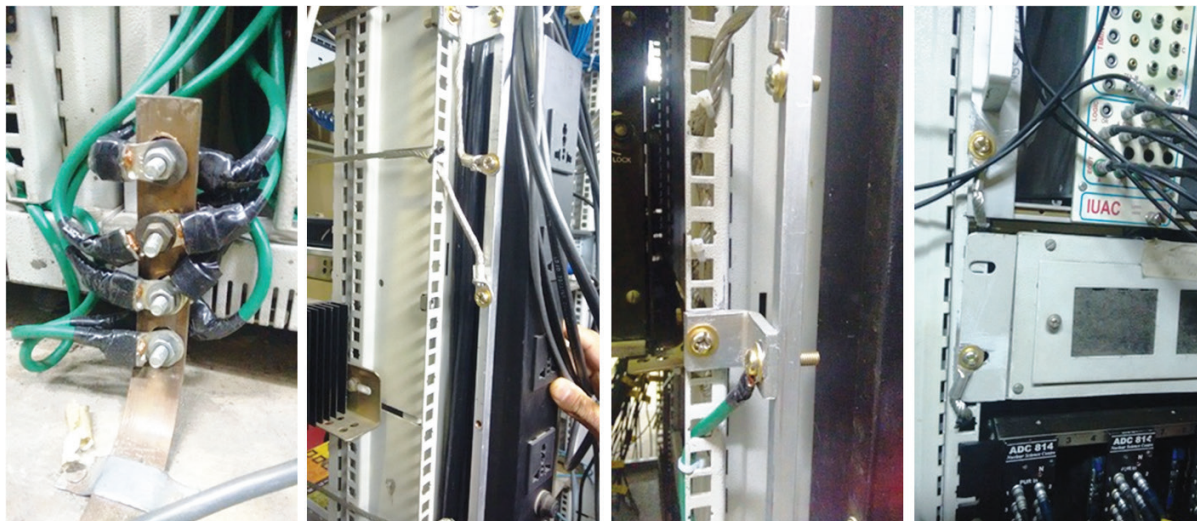


Fig. 4.2.2: Clean ground connections for INGA racks, crates and NIM bins.

#### 4.2.1.2 Repair of ACS high voltage distribution and preamplifier boxes

Some of the ACS high voltage distribution boxes were not working due to short circuit inside, (Figure 4.2.3). The damaged variable pots and cables were replaced and re-soldered. In some of the ACS preamplifier boxes there was no output which required re-soldering of the cables.

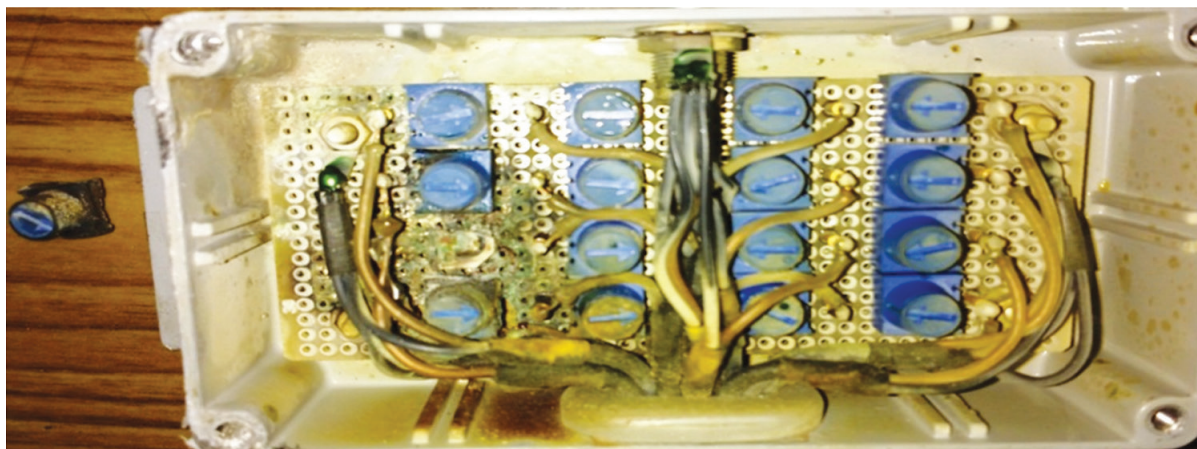


Fig. 4.2.3: ACS high voltage distribution box with damaged variable pot and cables.

We performed a test run with the INGA setup in April 2016. A beam of  $^{18}\text{O}$  of energies 100 and 90 MeV was bombarded on natural Ag target. The target was about  $2\text{mg}/\text{cm}^2$  thick, backed by a gold foil of thickness of about  $7\text{mg}/\text{cm}^2$ . During the test run, data was collected with a condition of two-fold coincidence of Compton suppressed Clover detectors. We collected data at a rate of about 8kHz with bit-pattern enabled data read-out. The dead-time at this rate was found to be insignificant. The experiments with INGA would start in the coming months.

### 4.2.1.3 Installation of ancillary devices in INGA:

R. Garg, S. K. Saini, R. Kumar, S. Muralithar, R. P. Singh and students from universities

Efforts are also on to couple ancillary devices with INGA. Mount for two Low Energy Photon (LEPS) detectors are also built in the workshop along with arrangement to mount BGO multiplicity filter detectors. The Plunger setup for INGA is ready and is waiting a beam test.

### 4.2.2 Charged Particle Detector Array

R. Kumar, Arti Gupta, Thomas Varughese and S. Venkataramanan

A  $4\pi$ CsI (TI) multi-detector Charged Particle Detector Array (CPDA) is being set-up for the detection of light charged particles such as protons and alpha particles, generated in heavy ion induced reactions. The array consists of CsI (TI) crystals each having an area of  $20\text{ mm} \times 20\text{ mm}$  with a thickness of 3 mm. The crystals are coupled to  $10\text{ mm} \times 10\text{ mm}$  photo-diode (model no. S-3590-08 supplied by Hamamatsu) via square-shaped (un-tapered)  $20\text{ mm} \times 20\text{ mm} \times 7\text{ mm}$  thick Plexi glass light guide. The front surface of the CsI crystal is covered with a 2  $\mu\text{m}$  mylar, aluminized on both the sides. The assembled units, model no. V20PM3/10-Cs, have been supplied by Scionix, Netherlands. The TI doping concentration is approximately 0.1 mol%. CPDA is being developed to serve as an ancillary detector system for INGA. The proposed array will have a Rhombicuboctahedron shape.

First prototype of charge sensitive preamplifier with minimum power dissipation (25mW per pre-amplifier) has been evaluated for this purpose and was successfully tested with CsI crystal. Resolution of 4.4%, 12.6%, and 6.9% were obtained using  $^{241}\text{Am}$  alpha source (Figure 4.2.4),  $^{137}\text{Cs}$  (Figure 4.2.5) and  $^{60}\text{Co}$  (Figure 4.2.6) sources, respectively.

**Table 1: Details of the sources used for the testing.**

Source	Type	Energy(MeV)	Resolution
$^{241}\text{Am}$	Alpha	5.486	4.4%
$^{137}\text{Cs}$	Gamma	0.662	12.6%
$^{60}\text{Co}$	Gamma	1.332	6.9%

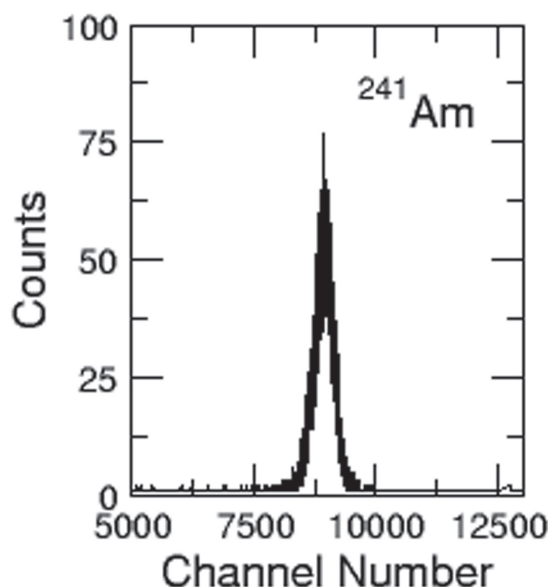


Fig. 4.2.4: Alpha Source -  $^{241}\text{Am}$ , resolution at 5.486 MeV is 4.4%.

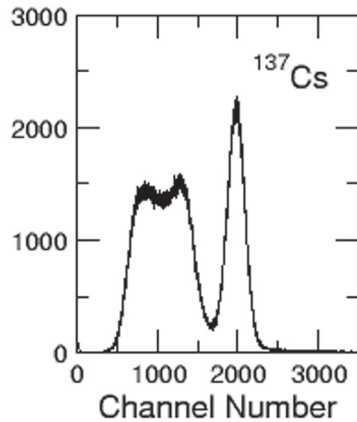


Fig. 4.2.5: Gamma Source- $^{137}\text{Cs}$ , resolution at 0.662 MeV is 12.6%.

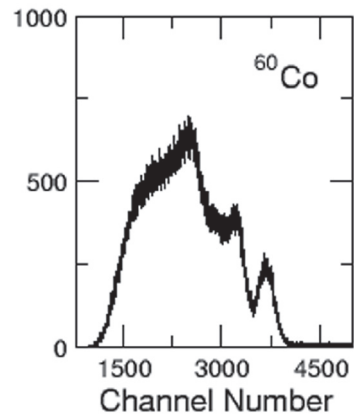


Fig. 4.2.6: Gamma Source- $^{60}\text{Co}$ , resolution at 1.332 MeV is 6.9%.

The entire array will be housed inside a hollow aluminium chamber of thickness 5mm. First prototype of this chamber is ready. Figure 4.2.7 and Figure 4.2.8 show the chamber and the Rhombicuboctahedron structure housed in it.



Fig. 4.2.7: Photograph of the vacuum chamber.

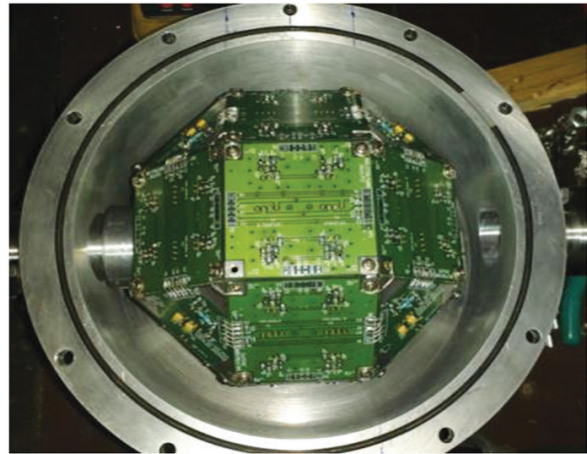


Fig. 4.2.8: Inside view of the chamber.

#### 4.2.3. Annealing of HPGe detectors

R. K. Gurjar, S. Muralithar, R. Garg, R. P. Singh and students from universities

Clover detectors with energy resolution worse than 3 keV at 1408 keV were annealed using the annealing setup at IUAC. Detectors with poor vacuum were pumped down to about  $10^{-7}$  Torr using the same setup. A picture of the set-up is shown in Figure 4.2.9.

#### 4.2.4. Experiments with GDA:

I. Bala, R. Kumar, A. Jhingan, S. Muralithar, R. P. Singh and university groups

GDA set up was used to study the variation of reduced transition probabilities in Sn isotopes through Coulomb excitation using Ni beam. A large area



Fig. 4.2.9: A Clover detector in the annealing setup.

annular multi-wire proportional counter was mounted at forward angles to detect the Coulomb scattered ions. GDA setup was also used for the study of incomplete fusion reactions for different target-projectile combinations. These experiments used recoil catcher activation technique followed by off-line gamma ray spectroscopy using HPGe detectors.

### 4.3 RECOIL MASS SPECTROMETERS AT IUAC

#### 4.3.1. Heavy Ion Reaction Analyzer (HIRA)

S. Nath, J. Gehlot, T. Varughese, A. Jhingan and N. Madhavan

HIRA was used in a student thesis experiment (Delhi University), to select the transfer reaction products formed in  $^{28}\text{Si} + ^{92,96}\text{Zr}$  system in order to probe channel coupling effects. The target-like products were separated from the primary beam as well as from scattered beam-like components using HIRA, positioned at  $6^\circ$  with respect to beam direction. The back-scattered projectile-like particles were detected in a two-dimensional, position sensitive silicon detector of  $25\text{ mm} \times 25\text{ mm}$  (with active area used  $\sim 21\text{ mm} \times 21\text{ mm}$ ). The back detector was mounted on an annular ring which could be rotated for coincidence optimization. A set of 13 BGO detectors (7 and 6 numbers above and below the horizontal reaction plane, respectively) in castle geometry were used for a possible triple-coincidence to quantify transfer to the excited states relative to those to the ground state.

The results of an earlier experiment to look for the effects of  $\beta_2$  and  $\beta_4$  values of the target nucleus on sub- and near-barrier fusion cross-sections using the systems  $^{16}\text{O} + ^{174,176}\text{Yb}$  have been published. Some new experiments have been proposed and/or sanctioned beam-time in the two AUC meetings for the utilization of HIRA in fusion and transfer reactions around barrier.

A new, large area MWPC detector has recently been assembled and preliminary tests have been carried out successfully using alpha particles from  $^{241}\text{Am}$  source. All the signals are found well above the noise (Figure 4.3.1). Detailed tests will be carried out for position resolution in X and Y before using at the focal plane of spectrometer. This addition would allow us to have a complete ray-tracing setup at the focal plane of spectrometer (HIRA or HYRA).

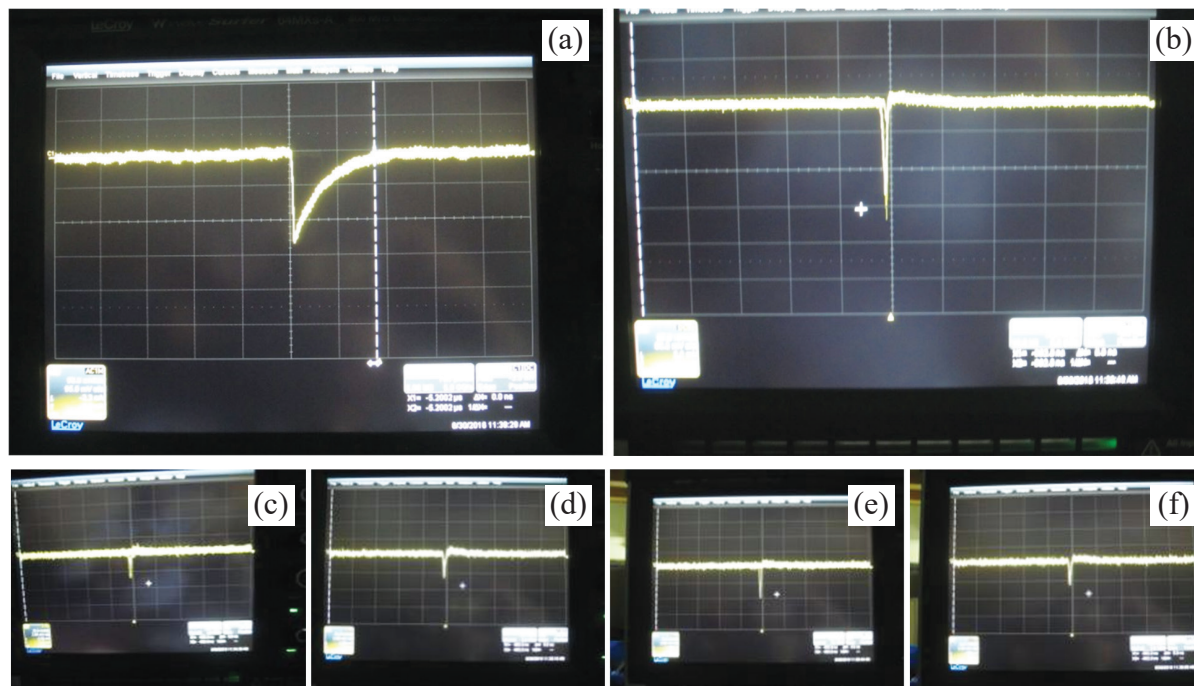


Fig. 4.3.1: Signals from the MWPC, tested with  $\alpha$ -particles from  $^{241}\text{Am}$  – (a) cathode, (b) anode, (c)  $X_{\text{left}}$ , (d)  $X_{\text{right}}$ , (e)  $Y_{\text{up}}$  and (f)  $Y_{\text{down}}$ .

### 4.3.2 HYbrid Recoil mass Analyzer (HYRA)

N. Madhavan, S. Nath, J. Gehlot, T. Varughese and A. Jhingan

Several experiments performed using HYRA first stage in gas-filled mode using LINAC beams, which had an overlap with this academic year, had already been reported in last year's annual report. Analysis carried out using the earlier year's evaporation residue (ER) cross section and spin distribution data show effects of both deformation and shell closure in  $^{48}\text{Ti} + ^{142,150}\text{Nd}$ ,  $^{144,154}\text{Sm}$  systems while for the  $^{32}\text{S} + ^{184}\text{W}$  system DNS model seem to reproduce experimental ER cross-sections.

Details of a new isomer identified in  $^{195}\text{Bi}$  (and present above a known isomer in that nucleus), using HYRA gas-filled mode, have been published. The excellent result obtained from this first experiment on isomer search/study using HYRA has encouraged us to build a dedicated isomer decay setup (Figure 4.3.2) at the focal plane (FP) of HYRA. The setup can accommodate up to 6 Clover germanium detectors at  $90^\circ$  and one along the direction of the products just behind the silicon 'stop' detector. The last detector and its mounting assembly can be dismantled to access the ER detectors. After detailed design, the setup is being fabricated and is expected to be ready for commissioning by this year end.

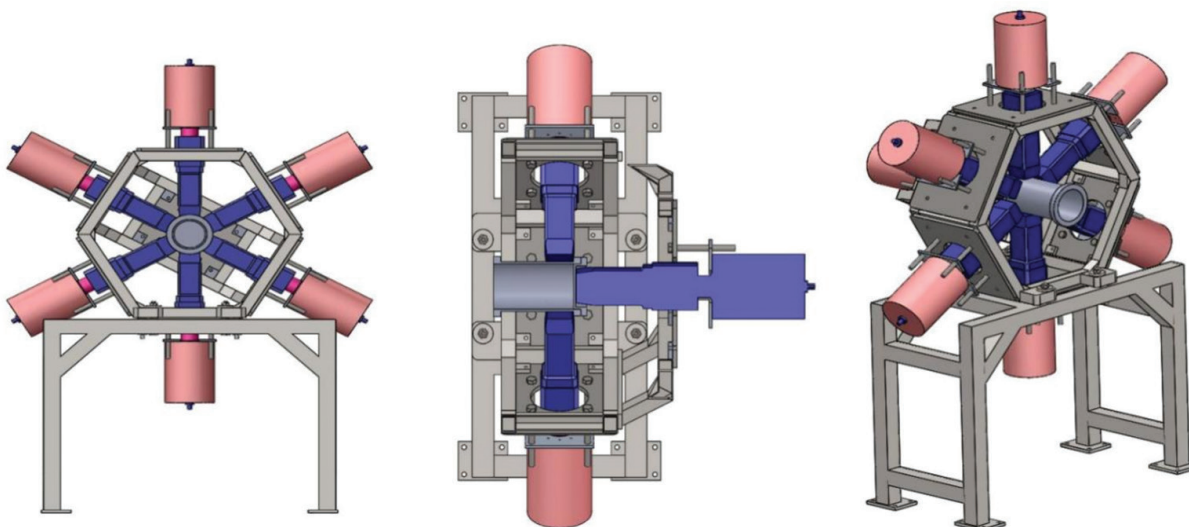


Fig. 4.3.2: Design of dedicated isomer decay setup for HYRA focal plane (cross-sectional and full view).

HYRA first stage was used in vacuum, momentum achromat mode, in a facility test experiment, in order to separate  $^{16}\text{O}$  reaction products from the primary beam of  $^{18}\text{O}$  (interacting with an aluminium target) and to look at coincidences with neutrons at forward angles. This was a trial run for a difficult experiment to distinguish between 'clustering' and 'pairing' processes. A fixed slit of dimensions 20 mm (in X) and 60 mm (in Y) was used at the centre of the split-quadrupole Q3 to reject the primary beam. A  $2\text{ cm} \times 2\text{ cm}$  pin-diode detector was used at the focal plane to detect the forward moving particles using energy and time-of-flight (TOF) with respect to the pulsed beam. Though the first stage of HYRA consists of only magnetic elements, the ions reaching the focal plane could be separated into different groups (of charge states) of  $^{16}\text{O}$ , scattered  $^{17}\text{O}$  and scattered  $^{18}\text{O}$  ions using energy and TOF signals, while the primary beam of  $^{18}\text{O}$  was completely stopped at the mid-plane of Q3. Coincidences between  $^{16}\text{O}^{8+}$  group and 'OR' of the six neutron detectors could be established. The actual experiment will be performed in inverse kinematics requiring coincidences between  $^{16}\text{O}$  ions detected at the focal plane and each individual neutron detector, for angular distribution, which may limit statistics and introduce additional challenges.

#### **4.4 MATERIALS SCIENCE FACILITY**

A. Tripathi, K. Asokan, V. V. Sivakumar, FouranSingh, S. A. Khan, P. K. Kulriya, I. Sulania, R. C. Meena, P. Barua, A. Kothari and D. K. Avasthi

The materials science facilities continue to support the research programmes of a large number of users from different universities and institutions. A total of 58 user experiments over 192 shifts were performed using the materials science beam line in beam hall I this year and there was no major loss of beam time due to facility breakdown. These included 21 runs spread over 71 shifts which were BTA experiments associated with students' Ph.D. programmes. The swift heavy ion (SHI) irradiation and related experiments were mostly performed in the radiation chamber of the materials science beam line in beamhall I. However, 4 experiments running over 21 shifts, including those utilizing in-situ XRD facilities, were performed in materials science beam line in beamhall II. Four more experiments spanning over 21 shifts, which mainly required low fluence irradiation, were performed in GPSC. Experiments were done in areas of SHI-induced materials modification and characterization and the details are given in Section 5.2.

The users also utilized various synthesis techniques and offline characterization facilities such as XRD, AFM, SEM, Raman, UV-Vis, I-V, Hall measurement etc. for characterizing more than 1500 samples. The testing for in-situ Moke chamber in beamhall I was completed and is ongoing in beamhall II. A new Gobbel mirror for thin film measurements was ordered to improve the efficiency of the XRD system. A new Hitachi UV-Visible-NIR Spectrophotometer with transmission and reflection mode was also installed.

##### **4.4.1 Maintenance of irradiation chambers in beam hall I**

S. A. Khan, R. C. Meena, A. Tripathi and S. K. Saini

The hydraulic lifting mechanism of the high vacuum chamber developed a problem in downward movement in December 2015. Hence, a local service engineer was called for repair of the same and the problem was rectified. The beamline was used by a large number of materials science users and 50 experiments spanning over 150 shifts were performed in this chamber.

##### **4.4.2 Online elastic recoil detection analysis and online residual gas analysis setups**

S. A. Khan and A. Tripathi

These systems were not utilized in any experiments in this period.

##### **4.4.3 Scanning Probe Microscope**

Indra Sulania and A. Tripathi

About 280 samples from 30 users were characterized with AFM in different modes. MFM was performed on 20 samples from 3 users. C-AFM was tried on 2 samples from 1 user and Tapping AFM was carried out for about 260 samples from 28 users.

The AFM facility ran satisfactorily throughout 2015 after repair of the mirror assembly. A problem with the sample alignment system of the scanner set-up was fixed with our own efforts.

##### **4.4.4 Field Emission Scanning Electron Microscope (FE-SEM)**

S. A. Khan, Sunil Kumar and A. Tripathi

TESCAN MIRA II LMH scanning electron microscope at IUAC is extensively utilized for users for characterizing various types of materials. This microscopy was performed for 101 users, this year, to study surface morphology of 434 samples and compositional analysis of 243 samples in EDX mode.

Many users have insulating samples on which a conducting coating is deposited using Quorum Technologies Q150TS sputter coater. The coater was used to deposit thin metal film on 205 such samples from 42 users in this year.

The gas flow tube in the coater was re-fixed inside the instrument after it had got completely removed due to high Argon gas flow. The electron emitter of FESEM is nearing its end. Hence, purchase of a new emitter is underway. SEM computer developed a problem in its motherboard which was rectified by the local vendor in a couple of days.

#### 4.4.5 Status report on spectroscopy facilities

Fouran Singh, Subodh K. Gautam, U. B. Singh, Arkaprava Das, S K Saini and P. Barua

The characterizations using spectroscopy techniques are very critical for deeper understating of the nature of materials including their modifications by ion beams. Some of such facilities like micro-Raman (MR), photoluminescence (PL), ionoluminescence (IL) and UV-visible spectroscopy are in operation for regular experiments. Recently, UV-Vis-NIR spectrometer has been installed and tested. The same will be soon available for regular user experiments. Solar simulator facility is also being implemented with funding from DST, which can be utilized for the characterizations of solar cells. The MR facility has been exploited by a large number of users from various universities and institutes. Successful experiments have been conducted on ion-irradiated oxide semiconductors, graphene, ferrites and other pervoskites including multiferroic materials and thin films. This facility can also be used as in-situ characterization of materials during the swift heavy ion (SHI) irradiation in beam hall-II. However, the scattering intensity from such materials should be enough to collect the signal using the fibre optic probe. PL facility is fully operational and being used regularly under blue (441.6 nm) and UV (325nm) excitations of HeCd laser. A series of successful IL experiments were also performed.

#### 4.4.6 Thermal evaporation and RF parallel plate diode sputtering systems

V. V. Siva Kumar

The RF parallel plate diode sputtering system, which had earlier been used to grow thin films of oxide materials, was changed to thermal evaporation system while the DC sputtering system having an asymmetric Cathode – Anode geometry, was changed to RF sputtering system. However, a parallel plate diode configuration was incorporated into the Microwave/ECR CVD system to enable the growth of thin films by RF sputtering with symmetric Cathode – Anode geometry and thin film depositions were performed with it for some users. Additionally, this set-up has the provisions to apply a DC bias to the substrate holder during deposition of thin films. The thermal evaporation system was used to study the growth of Aluminium nanorods (Al NRs) by oblique angle deposition (OAD) (Figure 4.4.1: left). While the SEM image (Figure 4.4.1 centre) of thin films grown with normal deposition showed formation of nanocrystals, their lateral growth and coalesce into film, SEM image (Figure 4.4.1: right) of thin films grown with OAD showed growth of Al NRs, i.e. self-shadowing effect caused vertical growth of nanostructures. The 100 A, 8 V power supply meant for Tungsten filament was upgraded to 200 A, 8 V to use evaporation boat also for thin film deposition. A thickness / rate monitor (Sycon Instrument, STM-100 M/F) was installed and tested during deposition of thin aluminium films of 125 nm having resistance less than 8  $\Omega$ .

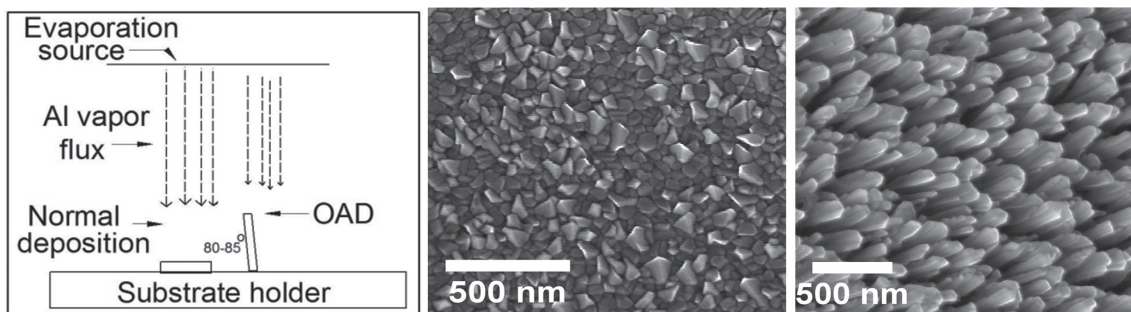


Fig. 4.4.1: (left) Schematic for normal and oblique angle depositions, (centre) SEM image of film grown with normal deposition and (right) SEM image of Al NR formed by OAD.

#### 4.4.7 Experimental set up for temperature dependent high resistance measurements

Ramcharan Meena, Shammi Verma, P. Kumar and K. Asokan

An experimental set-up for measuring the high resistance is developed using the Keithley Electrometer model 6517B. The basic principle of this is that it applies a certain amount of DC voltage and measures the current. The voltage range which can be applied through this is from 0 V to 999 V and the current which it can measure is in the range of 20 mA to 20 pA. The circuit diagram is shown in Fig. 4.4.2. Using this electrometer one can also measure the pyro-current, which is currently being planned.

The photograph in Figure 4.4.3 shows the measured value of the standard 1 G $\Omega$  resistance from WELWYN Components Limited. The measurement was performed with 10% tolerance.

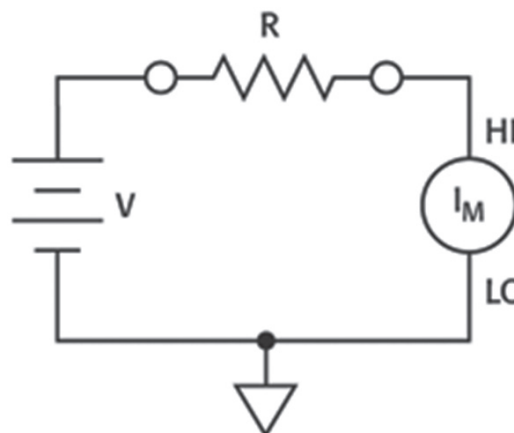


Fig. 4.4.2: The circuit diagram of high resistance measurement set-up.



Fig. 4.4.3 Photograph showing standard resistance.

Using this facility the temperature dependent resistance was measured for NiFe<sub>2</sub>O<sub>4</sub>. The result is shown in Fig. 4.4.4.

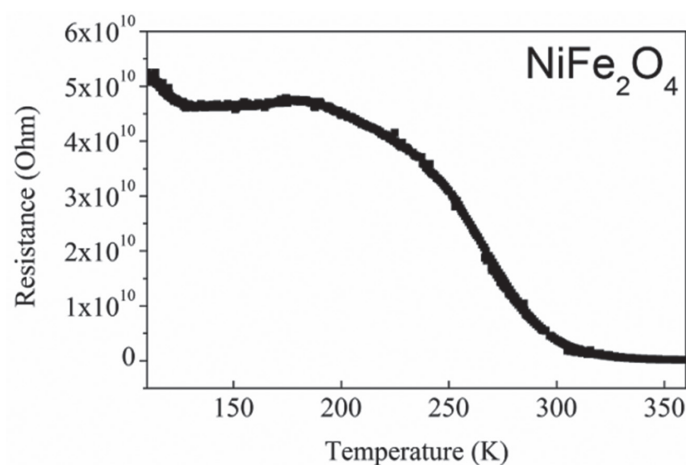


Fig. 4.4.4 Resistance vs Temperature graph for NiFe<sub>2</sub>O<sub>4</sub>.

## 4.5 RADIATION BIOLOGY EXPERIMENTAL FACILITY

A. Sarma

Different radiation biology experiments are being carried out in the dedicated radiation biology beam line of IUAC utilizing ASPIRE [Automated Sample Positioning and Irradiation system for Radiation biology Experiments], in which irradiations of cells can be done with a set of pre-set doses. The system is characterized by the dose uniformity over a field of 40 mm diameter within 2% standard deviation. The mean fluence is within 1 % of the electronically measured value at the centre of the field. The characterization of the system has also been done using irradiating SSNTD [CN 85].

The radiation biology laboratory is having the following equipment to facilitate the sample preparation and post irradiation treatments.

- Two CO<sub>2</sub> incubators, two biosafety cabinets, one small laminar flow bench for cell culture
- Field inversion gel electrophoresis, normal gel electrophoresis, protein gel electrophoresis set up
- Image-based cell counter [Invitrogen] which also gives information about cell viability and Beckman-Coulter Z<sub>2</sub> cell counter
- PCR machine, a crude gel documentation system, UV-Vis spectrophotometer and a fluorescence microscope
- Perkin Elmer multimode plate reader, Eppendorf and Plastocraftrefrigerated centrifuge and a Biotek micro-plate washer.

The laboratory section has independent split air-conditioning (AC) supply isolated from the central AC system. The CO<sub>2</sub> supply to the twin incubators is done from outside the lab area, which facilitates the replacement of empty cylinder without disturbing the laboratory environment.

Regular work is going on in the laboratory on analytical procedures involving gene expression studies using PCR, western blot, fluorescence immunostaining studies etc. by the users.

## 4.6 ATOMIC PHYSICS FACILITY

### 4.6.1 A setup for studying the charge state fraction of post collisional Ions

D. Swami, S. K. Saini, C. Pal and T. Nandi

Knowledge of the post foil charge state distributions is always useful in selecting the beam energy for a particular charge state for an experiment with maximum yield [1]. For studying the post foil charge state fractions, we are developing a new technique involving an Inclined and Straight plate Electro Static Analyzer (ISESA) [2] in beam hall II (Figure 4.6.1), in which one plate is held parallel and the other is kept inclined at a certain angle relative to the beam axis. A small gap (10mm) between the two plates at the entry causes large deflections due to a high field and a large gap at the exit allows the ions escaping the field region without hitting the plate. The details can be found in the previous annual report [3].

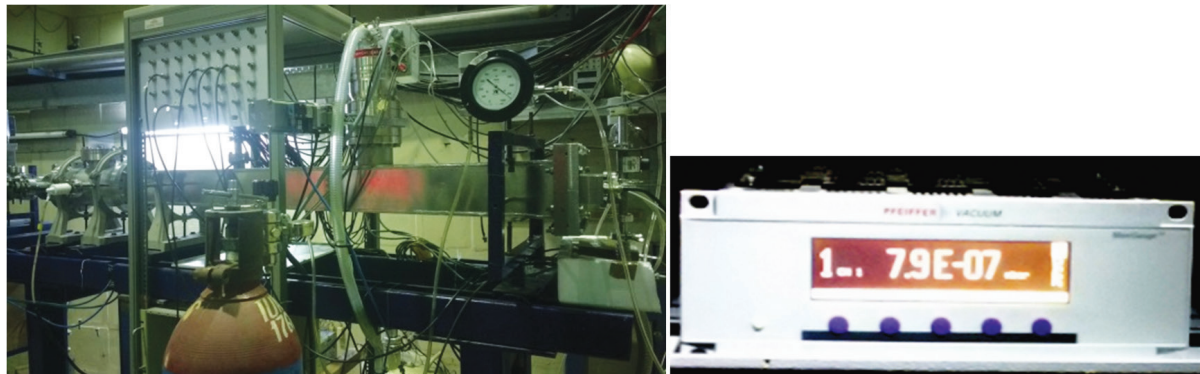


Fig. 4.6.1: ISESA set-up of atomic physics beam line.

The online test with the 55.7 MeV  $\text{Fe}^{+8}$  ion beam was performed last year. High noise in the position sensitive proportional counter (PSPC) spectra was noticed. Surprisingly, the noise persisted even without the beam, but it disappeared if the bias was put off. After thorough investigation, including better rounding-off of the edges of both electrodes, new electrical grounding, Teflon sleeving on the electrodes and changing of the cathode plate of the PSPC, the offline test with the  $^{55}\text{Fe}$  radioactive x-ray source showed no noise at all. Next online test will be conducted as per availability of the beam.

**REFERENCES:**

- [1] K. Shima, N. Kuno and M. Yamanouchi, *Phys Rev A* **40**, 7 (1989).
- [2] T. Nandi, N. Ahmad, H. K. Singh, and R. G. Pillay, *Rev. Sci. Instrum.* **75**, 11 (2004).
- [3] D. K. Swami, S.K. Saini, C. Pal and T. Nandi, *IUAC Annual Report*, Sec. 4.6.1 (2014-2015).